ARID ZONE JOURNAL OF ENGINEERING, TECHNOLOGY & ENVIRONMENT
AZOJETE December 2022. Vol. 18(4):721-728
Published by the Faculty of Engineering, University of Maiduguri, Maiduguri, Nigeria.
Print ISSN: 1596-2644, Electronic ISSN: 2545-5818
www.azojete.com.ng

ORIGINAL RESEARCH ARTICLE

INFLUENCE OF TUNGSTEN INERT GAS WELDING ON HARDNESS, TENSILE STRENGTH AND MICROSTRUCTURES OF ALUMINUM 6061 ALLOY WELDMENTS

A. A. Musa[1,2]*, M. A. Mohammed[1] and E. T. Dauda[1]
[1]*Department of Metallurgical and Materials Engineering, Ahmadu Bello University, PMB 1045, Zaria, Nigeria*
[2]*Department of Materials Science and Engineering, African University of Science and Technology, Abuja-Nigeria.*
**Corresponding author's email address: amusa@abu.edu.ng*

ARTICLE INFORMATION

Submitted 17 March, 2022
Revised 5 July, 2022
Accepted 10 July, 2022

Keywords:
TIG welding
Tensile strength
Hardness
Aluminium 6061 alloy
Microstructure

ABSTRACT

In this work, tungsten inert gas (TIG) welding was used for joining aluminum 6061 alloy because it offers low heat input to the weld joints and the ability to remove any refractory oxides such as Al_2O_3 through a process known as the cathodic cleaning effect. This research was carried out to evaluate the level of improvement in the tensile strength and the hardness of aluminum 6061 alloy welds, using a tungsten inert gas welding approach. Aluminum 6061 alloy in form of a round bar of length 100 mm and 8 mm in diameter was first machined to the standard tensile testing specimen according to the American society for testing and materials (ASTM) using a lathe machine. It was then butt welded along the center of the bar using tungsten inert gas welding process with a constant welding current of 18 Amperes and gas flow rate of 15 liter/min. the same process was repeated for both the hardness and microstructure specimens followed by butt welding along the center of the specimen. The welded samples were then subjected to the hardness and tensile testing using Rockwell hardness testing and Hounsfield tensile testing machine respectively. The results showed that the welded metal and the heat-affected zone possessed the highest hardness value of 84.2 HRB and 71.9 HRB respectively as compared with the parent metal with a hardness value of 66.8 HRB. Also, the tensile strength of the welded specimens is 300.35 N/mm² which is relatively lower than that of the base material with a tensile strength of 348.67 N/mm². Additionally, the results of the microstructural examination reveal the presence of trace aluminum oxides within the matrix of the welded structure which indicates the slight increase observed in the hardness of the welded sample as compare to that of the base material. Therefore, the hardness and tensile strength for the welded sample are close to the base metal indicating that welding of aluminum and its alloys using the TIG welding process gives welds of adequate mechanical properties.

1.0 Introduction

Welding is the method or technique by which metals are joined together by fusion, diffusion, or surface alloying through the application of heat or pressure, with or without a filler material (Musa *et al.,* 2020a). Welding involves many metallurgical phenomena and is considered one of the most effective methods of joining materials, despite its complex nature (Sergey *et al.,*

2020). These phenomena include melting, solidification, gas metal reaction, slag to metal reactions, surface effects, and solid reactions. A weldment comprises of weld metal zone, a heat-affected zone (HAZ), and the unaffected base metal. The structures of the weld metal usually differ from the base metal because it is composed of varying mixtures of filler material and base metal melted and solidified together during the welding process (Dauda, *et al.,* 2010; Sathiya *et al.,* 2012).

The weld metal and heat-affected zone must be compatible with the base metal if a successful and serviceable welded joint is to be produced. The filler electrode employed may be tailored to the mechanical properties and chemical composition of the metal but its structure could be markedly different. This structure and its attendant properties are a direct result of the sequence of events that occur just before and during the time the weld solidifies. These include reactions of the metal with gases in the vicinity of the weld, reactions with non-metallic liquid phase(s) (slag or flux) during welding, and solid-state reactions occurring in the weld after solidification (Dauda *et al*., 2010).

Aluminum and its alloys play an important role in most engineering applications due to their lightweight and excellent oxidation resistance, especially at high temperatures (Dursun and Soutis, 2014). The joining of aluminum and its alloy through the conventional arc welding processes has been very challenging due to its lower melting temperature and high activity with oxygen while in a molten state (Sathish *et al.,* 2021). Aluminum can be welded with ease by proper selection of the welding techniques as well as proper filler materials (Sadeghian and Iqbal, 2022). Tungsten inert gas welding (TIG) often referred to as gas metal arc welding (GMAW) is one of the commonly used arc welding processes for joining different materials used in critical industries such as construction, oil and gas, and pipeline industries (Vijayan and Seshagiri, 2018). It produces clean and high-quality welds joint and is suitable for joining very thin and medium thickness materials such as aluminum and its alloys, titanium and its alloy, low alloy steels, and stainless steels (Omiyale *et al*., 2022). This is because TIG offers lower heat energy input to the weld joint, thereby preventing burning or overheating of the weldment (Cibi and Thilagham, 2017; Musa *et al*., 2020b).

It istherefore important to study the structural changes that occur during gas tungsten arc welding of aluminum 6061 alloy to assess any significant variations in their hardness, tensile strength, and microstructural features when compared to the base metal (parent metal)

2. Materials and method

The materials used in this research are round aluminum 6061 Alloys and aluminum 5356 filler rods. The chemical composition of aluminum 6061 alloy and that of the filler rods are presented in Table 1

Table 1. Chemical compositions of both aluminium 6061 alloy and aluminium 5356 filler rod

	Percentage composition (%)	
Elements	Aluminium 6061 alloy	Aluminium 5356 filler rod
Cu	0.15-0.40	0.10
Mg	0.8-1.20	4.5-5.5
Mn	0.15	0.05-0.20
Si	0.40-0.80	0.25
Ti	0.15	0.060-0.20
Zn	0.25	0.10
Cr	0.04-0.35	0.050-0.25
Fe	0.7	0.40
Al	Balance	Balance

Corresponding author's e-mail address: jbhussein01@mautech.edu.ng

2.1. Method

Samples of Aluminium 6061 alloys were welded using tungsten inert gas welding process with aluminum 5356 filler rods to make a butt joint. Figure 1(a) shows the aluminium 6061 rods, while Figure 1(b) presents the aluminum 5356 filler rods. Welding of the samples was carried out using a gas tungsten arc welding machine (ARC-TIG AT101 INVERTER, manufacture by Orion AC&R Limited, United Kingdom). The welding parameters used were set at a constant current of 18 amperes and pure argon was used as the shielding gas at a constant flow rate of 15L/min. After welding of the specimens, they were allowed to cool and the welded specimens were machined carefully to avoid fracture by the aid of a lathe machine to the desired dimensions for the mechanical tests (hardness and tensile strength).

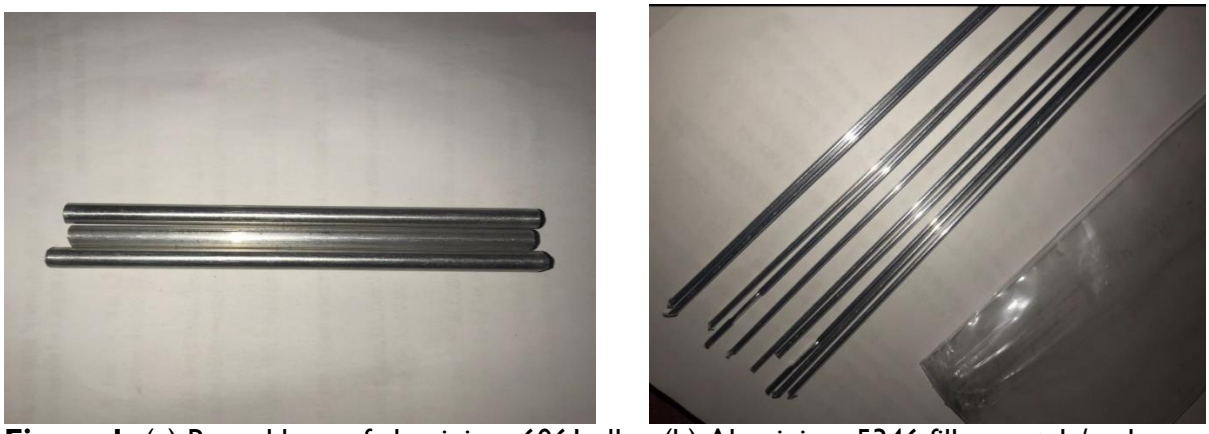

Figure 1: (a) Round bars of aluminium 6061 alloy (b) Aluminium 5346 filler metals/rods

2.2. The Tensile test

For the tensile test, the specimens were machined to desired dimensions for tensile testing using a lathe machine. The tensile test was carried out using a Hounsfield Tensometer (manufactured by British Rail Engineering Ltd, Swindon, England) to determine the behavior of the aluminum 6061 alloy welds under tension loading and to evaluate the ultimate tensile strength (UTS) as well as the percentage elongation after a fracture. The test consists of three samples that were subjected to tensile stress and the average of the results was taken for each set. The initial diameter for each specimen was measured with a vernier caliper the gauge length was also noted. A special graph sheet was used in the autographic recording drum to record and measure the relative motion of the drum and across the driving system, the percentage elongation and reduction was set to zero. The specimens were inserted into the tensometer using the split chucks and pins, precautions were taken to avoid too many marks. The load handle was rotated gently and uniformly until fracture of the specimen occurs. The final dimensions were then measured and the tensile strength was calculated using equation 1. Figures 2 and 3 showed the tensile test sample and the tungsten inert gas welding setup respectively.

$$\delta = \frac{P}{A} \qquad (1)$$

where: δ is the tensile strength (N/mm^2), P is the applied load in tension (N), A is the original cross-sectional area of the sample (mm^2).

Figure 2: Aluminium 6061 tensile test specimen as per ASTM standard

Figure 3: Tungsten inert gas welding setup

2.3 Hardness test

The welded and the unwelded specimens were used. The hardness of the specimens was measured using the Indentec Universal Hardness testing machine, model no-8187.5 LKV shown in Figure 4. This machine was manufactured by Indentec hardness testing machine Ltd. Zwick Roell, England. The indenter used 1/16-inch steel ball indenter and the scale was HRB. The specimens were mounted to enable them to sit properly on the machine. The load was then applied on the specimens and the indentation created on the surface of the specimen was then measured to determine their hardness, three readings were recorded and their average values were recorded.

Figure 4: Indentec universal hardness testing machine

2.4 Metallographic Examination

The microstructural examination was carried out on the welded samples and the base metal by using Optical Microscope (OPM) to reveal the microstructural changes due to heat energy input. The samples were passed through metallographic sample preparation to generate smooth and almost mirror-like surfaces of the specimens through the help of successive grinding and polishing processes using different sizes of grit papers (320,400,600,800) and polishing machine respectively. The grinding process was done in two stages which are the rough and fine stages; it was carried out with the addition of an adequate amount of water on top of the grit papers to avoid friction and overheating as well as damage to the ground surface After welding, the samples for investigation were prepared following the standard of the microscopic machine. The samples were first mounted in molds with epoxy resin for easy handling before grinding and polishing operation. The mounted samples were then passed

Corresponding author's e-mail address: jbhussein01@mautech.edu.ng

through a grinding operation using different grit papers as mentioned. During the grinding process, the direction of the samples was changed at the right angle when moving from the previous grit to the next finer grit paper. This is to remove the scratches produced by the previous grit papers and also, to maintain the microstructural integrity of the specimen. Polishing of the specimen's surface was then performed to achieve an almost perfect mirror-like surface. This was achieved by the aid of polishing cloth on a polishing machine that rotates and is electrically powered and to minimize the heat generation during polishing, changes in microstructure due to heat generation, polishing compound (Alumina) was used. The specimens were moved in an opposite direction to the motion of the machine to achieve the desired mirror-like surface. Finally, the welded and unwelded samples were etched to reveal the microstructural details that would otherwise not be evident on the polished sample. The etchant used for the aluminum sample was Keller's reagent which is mostly used for aluminum alloys, prepared with 190 ml distilled water, 5ml nitric acid, 2ml hydrofluoric acid, 3ml hydrochloric acid, the sample is immersed in the reagent after achieving mirror-polish surface for 10-30 seconds. Care was taken because this reagent contains 'HF' which can cause damages to glassware if it has direct contact with it. Therefore, it is often stored in an HDPE (high-density polyethylene) bottle. After proper etching, the specimens were then ready to be viewed under a metallurgical microscope to desirable magnifications of x100.

3. Results and discussion

3.1 Hardness

The hardness test result reveals that the weld metal (welded specimen) had the highest hardness with an average Rockwell hardness value of 84.2 HRB. The heat-affected zone showed a hardness value of 71.9 HRB, while the base metal (as-received sample) has a hardness value of 66.8 HRB as presented in Figure 5. The relative increase in the hardness values at the fusion and heat-affected zones of the weldment can be attributed to thermal cycles experienced during welding that may lead to the formation of the hardened ceramic phase of Al_2O_3 at these zones. The electric arc interacts with the material at the microstructural level during and immediately after welding which causes some phase transformations within the structure of the weldment which are mostly brittle phases, hence, making the hardness to be higher at the expense of its ductility and strength as reported in a study by Baghel and Nagesh (2018).

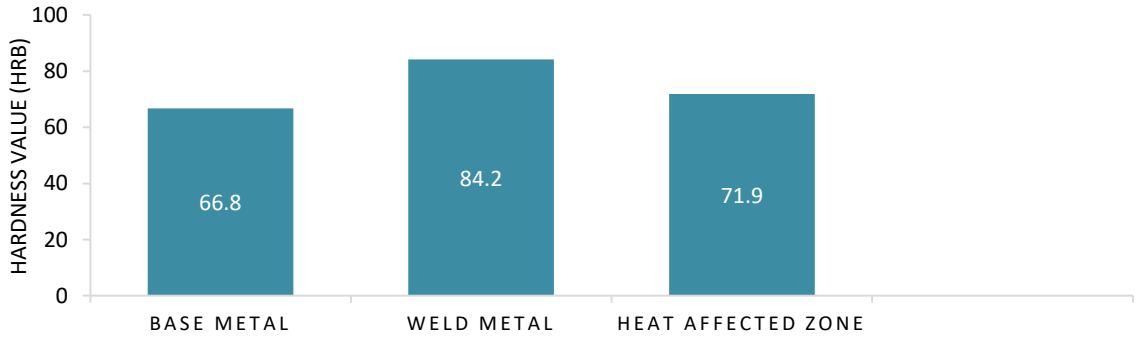

Figure 5: Rockwell Hardness tests results for base metal, weld metal, and heat-affected zone.

3.2 Tensile Test

Table 3 presents the tensile test results for both the welded and unwelded samples. It can be observed that the unwelded specimens possessed the highest tensile strengths with an average ultimate tensile strength (UTS) of 348.67 N/mm² with the corresponding percentage elongation of 25% after a fracture. While the welded samples showed an appreciable tensile

Corresponding author's e-mail address: jbhussein01@mautech.edu.ng

strength of 300.35 N/mm² with average percentage elongation of 13%. The decrease in the tensile strength of the welded sample may be attributed to the high-temperature gradient at the fusion zone and heat-affected zone which causes some microstructural changes such as brittle phase formations, hence lowering the tensile properties of the weldment, similar results have also been reported by Nazemi (2015).

Table 3: Tensile test results for both welded and unwelded samples

Experimental parameter	Unwelded sample	Welded sample
Original length (mm)	37	37
Gauge length (mm)	27	27
Fracture load (KN)	4.5	4.63
Ultimate tensile strength (N/mm²)	348.67	300.35
Maximum load (KN)	6.28	5.43
Elongation percentage (%)	25	13

3.3 Microstructural Examination

Microstructural characterization studies were conducted on metallographically prepared samples to investigate the morphological characteristics of both the welds and the base metal. Figure 6 shows the microstructure of the base metal of aluminum 6061 with white and black portions indicating the presence of aluminum and magnesium silicide (Mg_2Si) particles respectively. These particles were observed to be dispersed uniformly all over the aluminum matrix and are expected to be responsible for enhancing the properties like hardness and tensile strength hence, the reason for alloying aluminum with magnesium and silicon to form 6061 alloy as similarly observed by (Othman, 2011). Figure 7 showed the microstructure of the welded specimen having fine grains and dendritic structures which consists of traces of aluminum oxide precipitates within the structures of the weld metal. The presence of these phases is due to the thermal cycle that the welded joint has undergone during the welding process and without any post-weld heat treatment or modification done to the weldment after solidification. Figure 8 showed the heat-affected zone of the weldment with finer grains consisting of both aluminum oxides (Al_2O_3) and uniformly distributed magnesium silicide (Mg_2Si) particles. A similar result was previously reported by Rajiv and Gope (2015) and Liang (2018).

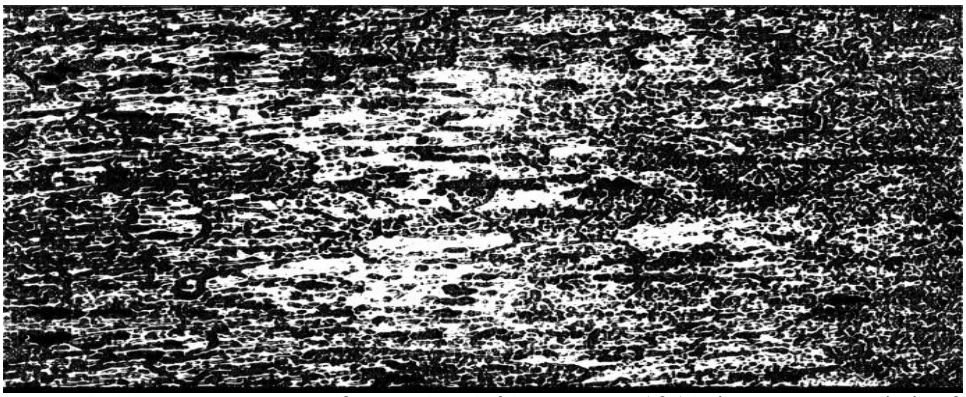

Figure 6: Microstructure of unwelded Aluminium 6061 (parent metal) (x100)

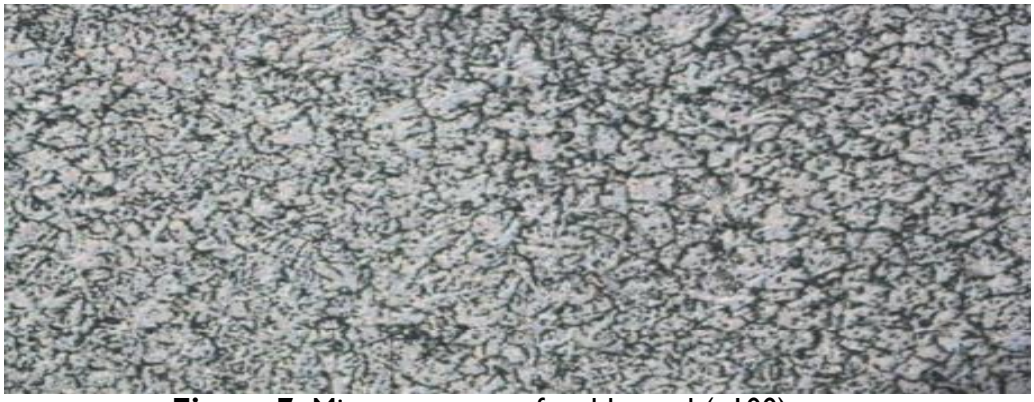

Figure 7: Microstructure of weld metal (x100)

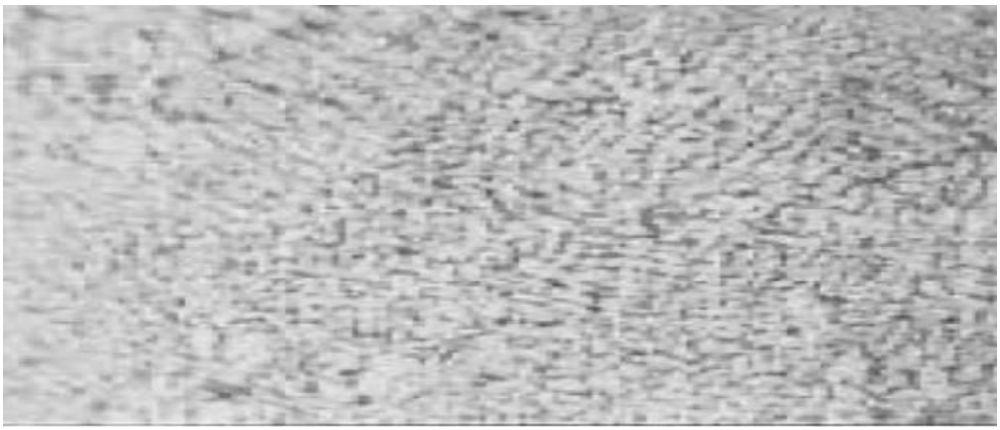

Figure 8: Microstructure of heat-affected zone (HAZ) (x100)

4. Conclusion

In this study, investigation of some mechanical properties and microstructural features of gas tungsten arc welding of aluminum 6061 alloy was carried out and the following conclusions were made:

- The parent metal showed the least hardness value with 14.61% lower as compared to that of the weld metal.
- The ultimate tensile strength of the welded sample is slightly lower with about 13.44% reduction as compared to that of the parent metal.
- The weld metal reveals coarse grain structures at the fusion and heat-affected zone of the weldment which causes the slight reduction in the tensile strength of the weld.
- Welding of Aluminium 6061 alloy using tungsten inert gas (TIG) process produced weld joints with improved properties that are closer to the properties of the parent metal.

Reference

Baghel, PK. and Nagesh, DS. 2018. Mechanical properties and microstructural characterization of automated pulse TIG welding of dissimilar aluminum alloy. Indian Journal of Engineering and Materials Sciences, 25: 147-154.

Cibi, AJ. and Thilagham, KT. 2017. High-Frequency Gas Tungsten Arc Welding Process for Dressing of Weldment. International Journal of Advanced Engineering Research and Science (IJAERS), 4(3): 229-235.

Dauda, ET., Hassan, SB., Aponbiede, O., Nyior, GB. and Mohammed, RA. 2010. The assessment of Microstructure and hardness characteristics of some welded low carbon steels. Nigerian Journal of Engineering, 17: 67-73.

Dursun, T. and Soutis, C. 2014. Recent developments in advanced aircraft aluminum alloys. Materials and Design 56: 862-871.

Liang, Y., Shen, J., Hu, S., Wang, H. and Pang, J. 2018. Effect of TIG current on microstructural and mechanical properties of 6061-T6 aluminum alloy joints by TIG–CMT hybrid welding. Journal of Materials Processing Technology, 255: 161-174.

Musa, AA., Dauda, ET. and Bello, KA. 2020a. Microstructural Features and Mechanical Properties of AISI 430 Ferritic Stainless Steel Welds - A Review. FUDMA Journal of Sciences (FJS), 4(1): 677–685.

Musa, AA., Dauda, ET., Bello, KA. and Adams SM. 2020b. Optimization of TIG Welding Parameters on the Tensile Strength Performance of Ferritic Stainless Steel Welds Using Response Surface Methodology. Indian Journal of Engineering, 17(48): 591-604.

Nazemi, N. 2015. Identification of the mechanical properties in the heat-affected zone of aluminum welded structures. Electronic Theses and Dissertations, University of Windsor, Ontario, Canada.

Omiyale, BO., Olugbade, TO., Abioye, TE. and Farayibi, PK. 2022. Wire arc additive manufacturing of aluminium alloys for aerospace and automotive applications: A review. Materials Science and Technology, 38(7): 391- 408.

Othman, NK., Bakar, SRS., Jalar, A., Syarif, J. and Ahmad, MY. 2011. The effect of filler metals on mechanical properties of 6mm AA 6061-T6 welded joints. Advanced Materials Research, 154(155): 873-876.

Sadeghian, A. and Iqbal, N. 2022. A review on dissimilar laser welding of steel-copper, steel-aluminum, aluminum-copper, and steel-nickel for electric vehicle battery manufacturing. Optics & Laser Technology, 146: 107595.

Sathish, T., Tharmalingam, S., Mohanavel, V., Ashraff, AKS., Karthick, A., Ravichandran, M. and Rajkumar, S. 2021. Weldability Investigation and Optimization of Process Variables for TIG-Welded Aluminium Alloy (AA 8006). Advances in Materials Science and Engineering, 28(16): 1-17.

Sathiya, P., Mahendra, KM. and Shanmugarajan, B. 2012. Effect of shielding gases on microstructure and mechanical properties of super austenitic stainless steel by hybrid welding. Materials and Design, 33: 203-212.

Sergey, S., Tri, Le-Q., Bastian, M., Farzad, VF., Margie, PO., Alexander, R., Giulio, M., Christian, L. and Kilian, W. 2020. Supervised deep learning for real time quality monitoring of laser welding with X-ray radiographic guidance. Scientific Reports https://doi.org/10.1038/s41598-020-60294-x. 10(1): 1-12

Vijayan, D. and Seshagiri, VR. 2018. Process Parameter Optimization in TIG Welding of AISI 4340 Low Alloy Steel Welds by Genetic Algorithm. IOP Conf. Series: Materials Science and Engineering, 390: 1-8. doi:10.1088/1757- 899X/390/1/01206